*Selected Papers*

# BODIPY-Based Ratiometric Fluoroionophores with Bidirectional Spectral Shifts for the Selective Recognition of Heavy Metal Ions

**Akira Hafuka,[1] Hiroki Taniyama,[1] Sang-Hyun Son,[2] Koji Yamada,[2] Masahiro Takahashi,[1] Satoshi Okabe,[1] and Hisashi Satoh*[1]**

[1]Division of Environmental Engineering, Faculty of Engineering, Hokkaido University, North-13, West-8, Kita-ku, Sapporo, Hokkaido 060-8628

[2]Section of Materials Science, Faculty of Environmental Earth Science, Hokkaido University, North-10, West-5, Kita-ku, Sapporo, Hokkaido 060-0810

Received August 30, 2012; E-mail: qsatoh@eng.hokudai.ac.jp

Two novel asymmetric BODIPY fluoroionophores with dipicolylamine (**BDP-DPA**, dipicolylamine: bis(pyridylmethyl)) and terpyridine (**BDP-TPY**) are described. These fluoroionophores display opposite wavelength responses on complexation with heavy metal ions. Furthermore, the fluorescence spectra vary depending on the ionic species. In particular, **BDP-DPA** shows a high affinity toward $Cr^{3+}$ and upon complexation, the fluorescence spectrum blue-shifts from 591 to 566 nm. In contrast, **BDP-TPY** preferentially binds to $Zn^{2+}$ and the fluorescence spectra red-shifts from 539 to 567 nm. **BDP-TPY** is the first example of asymmetric BODIPY with a pyridyl receptor at the 3 position showing red-shifted fluorescence by complexation with metal ions. The concentration of each metal ion was successfully determined by ratiometric measurement. The wavelength-responses characteristics of these fluoroionophores could be very useful in the development of novel ratiometric fluoroionophores for metal ions.

The conservation and protection of the natural environment from trace contaminants are becoming increasingly important, and in particular, heavy metals pose severe risks to human health and to the environment because of their toxicity.[1] For instance, chromium (Cr) is a common heavy metal contaminant used throughout the world, and its compounds can have genotoxic effects on humans and increase the risk of lung cancer.[2] It originates primarily from industrial uses, such as electroplating, metal finishing, and leather tanning.[3] Zinc (Zn) is also one of the major heavy metal pollutants because of its widespread industrial applications in chemical and alloyed products, fabricated metal products, and paper products.[4] Zn compounds have hazardous effects not only on humans but also on fish and plants.[5] Currently, the most common analytical methods for heavy metals are atomic absorption spectrometry (AAS) and inductively coupled plasma (ICP) spectroscopy.[6,7] Although precise, these analytical instruments are expensive and often require complex sample preparation. In addition, they are not applicable to continuous on-site monitoring and measure only the total concentration of heavy metals. Therefore, an inexpensive and simple method is needed for determining levels of heavy metal ions, which is appropriate for monitoring industrial and environmental samples.

Fluorescence spectroscopy is a desirable method for quantifying heavy metal ions because of its high sensitivity, operational simplicity, and versatile instrumentation.[8] The design and development of novel fluoroionophores remain an active area of research, and various fluoroionophores for heavy metal ions have been reported.[9–11] In terms of sensitivity, fluoroionophores that exhibit ratiometric spectral changes induced by complexation with heavy metal ions are more favorable than those exhibiting only fluorescence enhancement ("turn-on") or fluorescence quenching ("turn-off"). Ratiometric fluoroionophores provide more detailed information about the analyte in a sample, as well as allowing reliable measurements of the analyte concentration, as the ratio of the fluorescence intensities at two wavelengths is independent of fluctuations of the source light intensity and sensitivity of the instrument.[12] However, the development of ratiometric fluoroionophores is still challenging.

Our concept for the ratiometric measurement of heavy metal ions is based on the synthesis of an asymmetric 4,4-difluoro-4-bora-3a,4a-diaza-*s*-indacene (BODIPY) fluorophore which has an ion receptor at the 3 position. BODIPY fluorophores possess many valuable characteristics, such as sharp and intense absorption and fluorescence bands, high fluorescence quantum yields, high molar absorption coefficients, and good photochemical stability.[13] Furthermore, since BODIPY fluorophores are amenable to structural modification, controlling the substituent pattern allows for changes in the wavelength of the absorption and fluorescence spectrum.[14] Many BODIPYs for cations have been reported,[15–22] usually containing an amino group as a cation receptor at the 3 position of the BODIPY core. However, there are no studies on asymmetric BODIPY, which has a pyridyl ion receptor at the 3 position. In this study, we present 2,2′:6′,2″-terpyridine-substituted BODIPY (**BDP-**

Published on the web December 29, 2012; doi:10.1246/bcsj.20120235

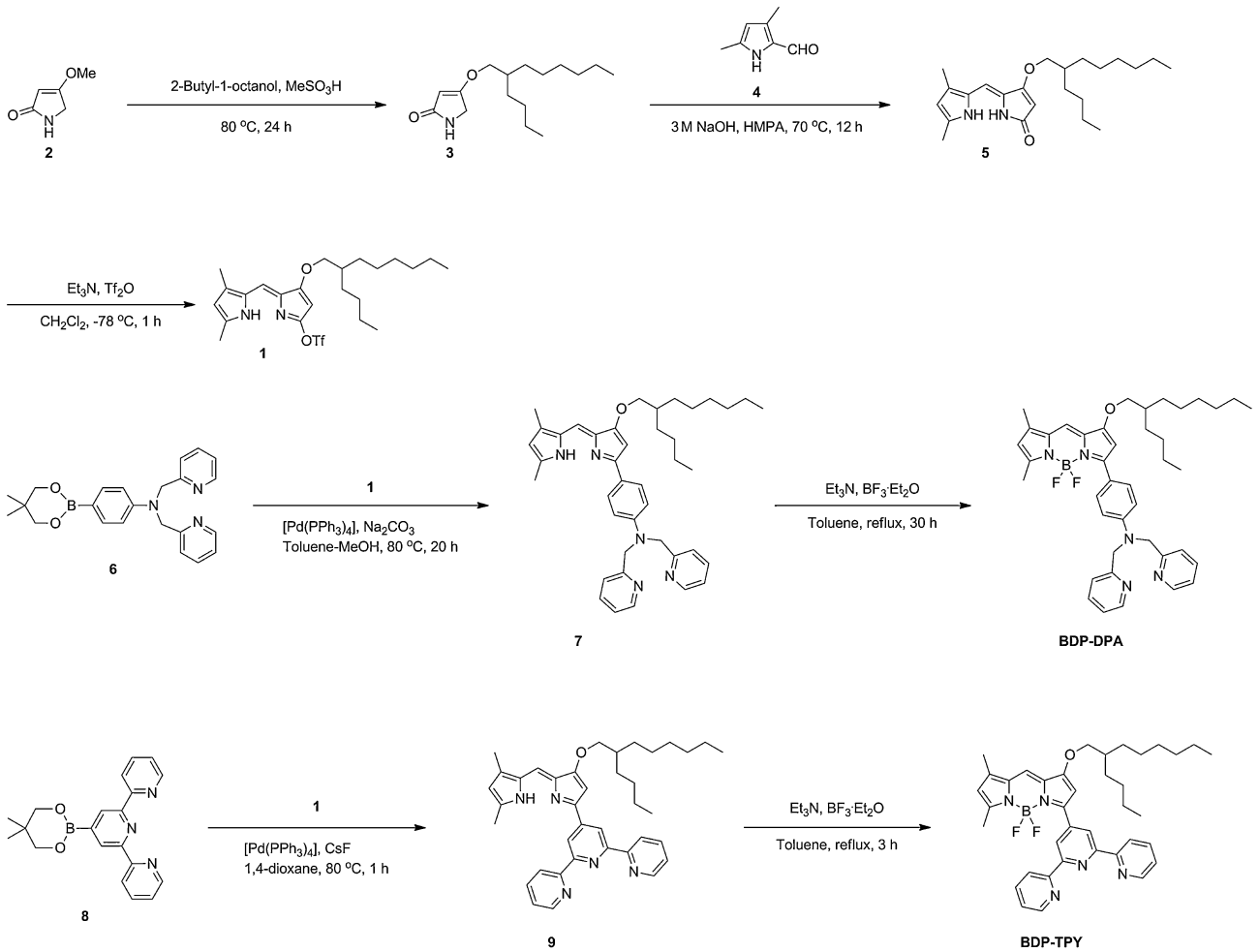


**Scheme 1.** Synthesis of **BDP-DPA** and **BDP-TPY**.

**TPY**) and di(2-picolyl)amine-substituted BODIPY (**BDP-DPA**, di(2-picolyl): bis(pyridin-2-ylmethyl)) as fluoroionophores for heavy metal ions. $Zn^{2+}$ and $Cr^{3+}$ ion concentrations were successfully determined by ratiometric measurement by using **BDP-TPY** and **BDP-DPA**, respectively. Interestingly, these fluoroionophores show opposite wavelength responses toward metal ions. Development of such diversified sensing fluoroionophores allows for identification of several heavy metal ions.

## Results and Discussion

**BDP-DPA** and **BDP-TPY** were synthesized according to the sequences summarized in Scheme 1. We chose two types of heavy metal ion receptors, namely di(2-picolyl)amine (DPA) and 2,2′:6′,2″-terpyridine (TPY), both of which are popular metal-ion receptors. However, their chemical properties are very different, that is, DPA is a strong electron-donating group in intramolecular charge-transfer systems, while TPY is a heterocyclic moiety in metal-to-ligand charge-transfer systems. DPA is well known as a chelator of metal ions and is widely used for the design of new fluoroionophores.[10,17,20,23–25] The terpyridine unit is an excellent general metal-ion binder. It is known that the terpyridine unit is able to coordinate with several kinds of metal ions with high binding constants especially $Zn^{2+}$.[26,27] In our synthetic scheme, the metal-ion receptor was directly linked to the 3 position of the BODIPY core using the Suzuki–Miyaura cross-coupling reaction. This synthetic method facilitates the production of not only an amino-group but also a pyridyl-group functional BODIPY using the common compound **1**.

Fluorescence and colorimetric titration experiments of **BDP-DPA** with different metal ions were carried out to clarify its ion sensing ability. Figure 1 shows the fluorescence spectra of **BDP-DPA** (1 μM) measured with and without each respective metal ion (500 equiv). Without the ions, **BDP-DPA** showed a magenta fluorescence around 591 nm with a low fluorescence quantum yield ($\Phi = 0.13$). The possible influence of interfering ions was also investigated. Upon addition of $Cr^{3+}$, $Fe^{2+}$, $Fe^{3+}$, $Zn^{2+}$, $Cd^{2+}$, $Hg^{2+}$, or $Pb^{2+}$, the spectrum shifted to shorter wavelengths. Interestingly, the extent of the spectral shift could be divided into three patterns, and fluorescence intensities varied depending on the ion species. $Zn^{2+}$ and $Cd^{2+}$ induced large hypsochromic shifts of the fluorescence band from 591 to 547 nm for $Zn^{2+}$ and to 549 nm for $Cd^{2+}$. In comparison, $Cr^{3+}$, $Fe^{2+}$, $Fe^{3+}$, and $Pb^{2+}$ showed relatively small blue shifts from 591 to 566 nm. $Hg^{2+}$ exhibited blue-shifted fluorescence at 560 nm. The blue-shifted fluorescence can be explained by an intramolecular charge-transfer (ICT)

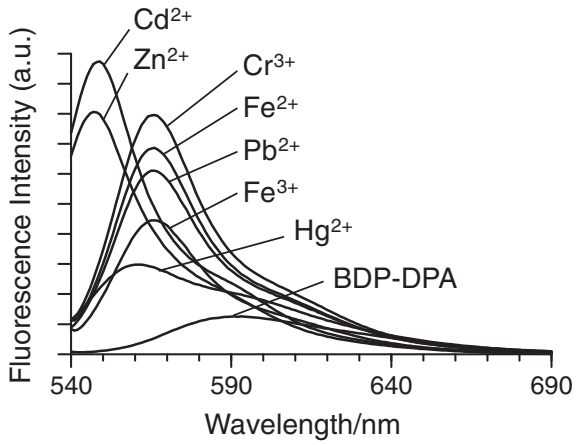


**Figure 1.** Fluorescence spectra of **BDP-DPA** in the presence of different metal ions (500 μM) in aqueous acetonitrile solution (acetonitrile/water = 9/1, v/v) with excitation at 535 nm. The concentration of **BDP-DPA** was 1 μM.

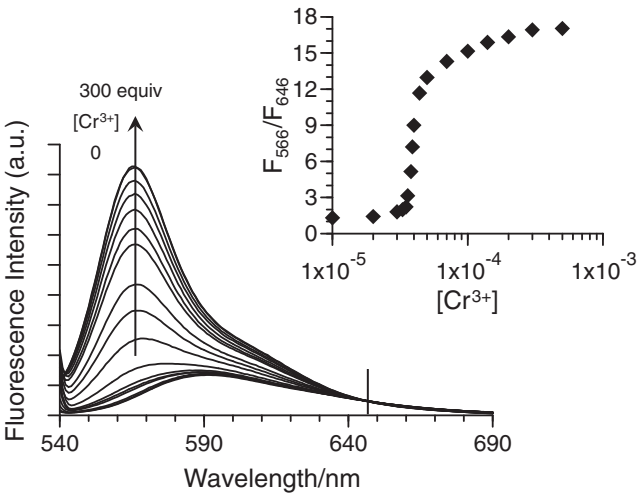


**Figure 2.** Changes in the fluorescence spectrum of **BDP-DPA** with $Cr^{3+}$ and plot of the fluorescence intensity ratio ($F_{566}/F_{646}$) of **BDP-DPA** versus increasing $Cr^{3+}$ concentration. Spectra are for $Cr^{3+}$ concentrations of 10, 20, 30, 33, 35, 36, 38, 39, 40, 44, 50, 70, 100, 200, and 300 μM. Spectra were acquired in aqueous acetonitrile solution (acetonitrile/water = 9/1, v/v) with excitation at 535 nm. The concentration of **BDP-DPA** was 1 μM.

mechanism.[28] When a fluoroionophore contains an electron-donating group (e.g., amino group) linked to a fluorophore, it undergoes ICT from the donor moiety to the fluorophore, resulting in red-shifted fluorescence.[12] Conversely, when coordinated with an ion, the amino group loses its electron-donating ability, and consequently ICT is inhibited and the fluoroionophore exhibits blue-shifted fluorescence. The fluorescence quantum yield of a fluoroionophore always increases in this process. These spectral changes allow ratiometric fluorescence measurements of the concentration of a metal ion. The ratiometric measurement of the fluorescence intensities at two appropriate fluorescence wavelengths provides a more reliable measurement of the analyte concentration than the measurement of the intensity at only a single wavelength. In the absorption spectra, **BDP-DPA** showed a sharp and strong absorption band around 549 nm ($\varepsilon = 56000$) in the same solvent system (Table S1). Upon interaction with 500 equiv of metal ions, a distinct change in the absorption spectrum of **BDP-DPA** was observed. Upon addition of heavy or transition-metal ions, the spectra showed a hypsochromic shift. In particular, the absorption band of **BDP-DPA** at 549 nm underwent a large hypsochromic shift to 517 nm upon addition of $Cu^{2+}$ (Table S1).

The fluorescence spectra of the concentration variable titration of **BDP-DPA** with $Cr^{3+}$ in an aqueous acetonitrile solution are shown in Figure 2. Upon addition of $Cr^{3+}$ to the solution, the fluorescence band of **BDP-DPA** shifted hypsochromically by 25 nm (from 591 to 566 nm). The fluorescence quantum yield increased from 0.13 to 0.48. An isoemission point was found at 646 nm, which renders the fluoroionophore useful for ratiometric measurements. To the best of our knowledge, this is only the second example of ratiometric sensing of $Cr^{3+}$.[29] The spectral change was almost terminated by the addition of 500 equiv of $Cr^{3+}$. Similar changes were observed in the absorption spectra. When $Cr^{3+}$ was added to the solution, the maximum absorbance shifted slightly from 549 to 537 nm with an isosbestic point at 542 nm (Table S1). The fluorescent intensity at 566 nm significantly increased with increasing concentration of $Cr^{3+}$, while the fluorescence intensity at 646 nm was unchanged. Therefore, the ratio of the fluorescence intensities at 566 to 646 nm ($F_{566}/F_{646}$) was calculated for ratiometric analysis. The $F_{566}/F_{646}$ changed as the $Cr^{3+}$ concentration was varied. When the $Cr^{3+}$ concentration was 500 equiv, the $F_{566}/F_{646}$ increased to 17.0, and the fluorescence color changed from magenta to yellow. As shown in Figure 2, the sigmoidal plot of $F_{566}/F_{646}$ versus the $Cr^{3+}$ concentration gives the useful range for quantitative determination of $Cr^{3+}$. The LOD and LOQ were $3.2 \times 10^{-6}$ and $1.1 \times 10^{-5}$ M for $Cr^{3+}$ in this aqueous solvent system, respectively. Moreover, the binding constant could be determined using Benesi–Hildebrand plots (Figure S1).[30] The result suggested a 1:1 stoichiometry for the **BDP-DPA**/$Cr^{3+}$ complex and the binding constant to be $3.94 \times 10^4\ M^{-1}$ for $Cr^{3+}$, which is relatively high compared to other $Cr^{3+}$ fluoroionophores.[31–35]

The selectivity of **BDP-DPA** to $Cr^{3+}$ was investigated with some common ions. Environmentally important metal ions, such as $Na^+$, $Mg^{2+}$, $K^+$, $Ca^{2+}$, and $Mn^{2+}$ did not increase the fluorescence intensity at 566 nm, which originates from the complex of **BDP-DPA** with Cr (Figure 3). The signal increased notably in other ion solutions. However, when $Cr^{3+}$ was added to these solutions, $F_{566}$ increased further. This indicates that **BDP-DPA** has a high affinity for $Cr^{3+}$. $Fe^{2+}$and $Fe^{3+}$ are the main competitive ions toward **BDP-DPA** as a $Cr^{3+}$ fluoroionophore because the fluorescence and absorption bands of these ion solutions overlap with those of $Cr^{3+}$. This result indicated that interaction between Fe ion and lone pairs of nitrogen atoms in a DPA unit may be similar to that of $Cr^{3+}$. However, the complex of $Cr^{3+}$ and **BDP-DPA** showed slightly higher fluorescence intensity than that of $Fe^{2+}$ and $Fe^{3+}$. $Cu^{2+}$ showed a fluorescence quenching effect on **BDP-DPA**, which has often been found for other metal-ion fluoroionophores due to energy/electron transfer (e.g., paramagnetic $Cu^{2+}$).[10,11,17,22,25,26,31,36]

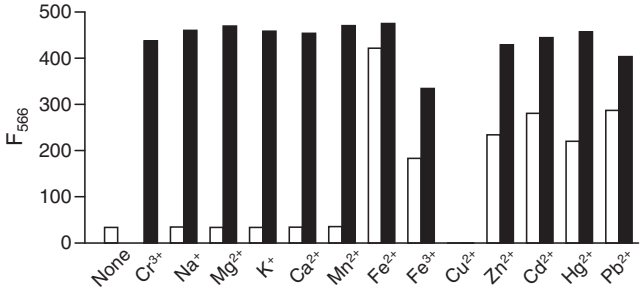


**Figure 3.** Changes in the fluorescence intensity ($F_{566}$) of **BDP-DPA** upon the addition of different metal ions. Spectra were acquired in aqueous acetonitrile solution (acetonitrile/water = 9/1, v/v). White bars represent the addition of an excess of the appropriate metal ion (1 mM for $Na^+$, $Mg^{2+}$, $K^+$, and $Ca^{2+}$. 500 μM for all other ions) to a 1 μM solution of **BDP-DPA**. Black bars represent the subsequent addition of 500 μM of $Cr^{3+}$ to the solution. Excitation was provided at 535 nm.

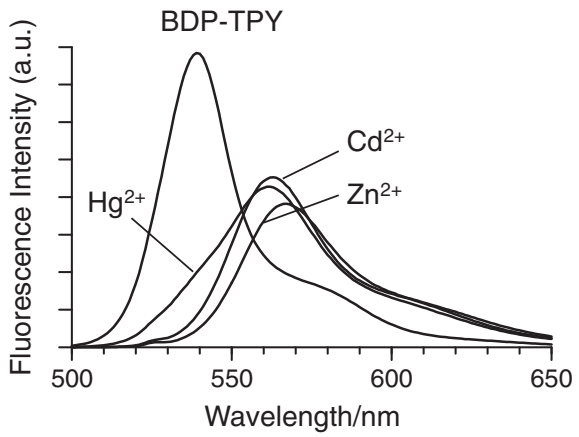


**Figure 4.** Fluorescence spectra of **BDP-TPY** in the presence of different metal ions (50 μM) in aqueous acetonitrile solution (acetonitrile/water = 9/1, v/v) with excitation at 525 nm. The concentration of **BDP-TPY** was 1 μM.

The response of **BDP-DPA** to variations in pH was investigated (Figure S2). The fluorescence bands around 591 nm originating from **BDP-DPA** were stable at pH 5.0, 7.0, and 9.0. Fluorescence enhancement was observed at pH 3.0 with a hypsochromic shift to 566 nm, which is possibly due to protonation of **BDP-DPA** under low pH conditions.[17,37,38]

Figure 4 shows the fluorescence spectra of **BDP-TPY** in an aqueous acetonitrile solution with and without the respective metal ions (50 equiv). Without the ions, **BDP-TPY** showed a greenish-yellow fluorescence at 539 nm with a high fluorescence quantum yield ($\Phi = 0.91$) and a shoulder around 580 nm, which is typical of BODIPY fluorophores.[39] In contrast to **BDP-DPA**, the spectra of **BDP-TPY** were shifted to longer wavelengths upon addition of $Zn^{2+}$, $Cd^{2+}$, and $Hg^{2+}$. The extent of the spectral shift depends on the ion species. Complexes of **BDP-TPY** with $Cd^{2+}$ and $Hg^{2+}$ showed red-shifted fluorescence bands at 563 and 561 nm, respectively, while $Zn^{2+}$ induced the largest bathochromic shift (from 539 to 567 nm) of the fluorescence band. Goze et al. reported that BODIPY fluoroionophores functionalized with terpyridine at

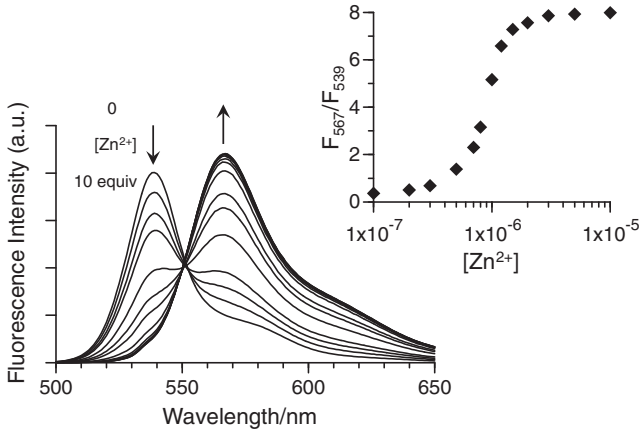


**Figure 5.** Changes in the fluorescence spectrum of **BDP-TPY** with $Zn^{2+}$ and plot of the fluorescence intensity ratio ($F_{567}/F_{539}$) of **BDP-TPY** versus increasing $Zn^{2+}$ concentration. The spectra shown are for $Zn^{2+}$ concentrations of 0, 0.1, 0.2, 0.3, 0.5, 0.7, 0.8, 1.0, 1.2, 1.5, 2.0, 3.0, 5.0, and 10.0 μM. Spectra were acquired in aqueous acetonitrile solution (acetonitrile/water = 9/1, v/v) with excitation at 535 nm. The concentration of **BDP-TPY** was 1 μM.

the meso position showed fluorescence quenching toward $Zn^{2+}$.[40] **BDP-TPY** is the first example of asymmetric BODIPY with a pyridyl receptor at the 3 position showing red-shifted fluorescence by complexation with metal ions. It is known that when electron-withdrawing groups (e.g., pyridyl group) are part of the fluorophore $\pi$-system and involved in ion binding, the excited state is more stabilized than the ground state upon complexation with metal ions, and therefore the energy gap is reduced.[41,42] In **BDP-TPY**, the terpyridine moiety could interact with metal ions in this way, resulting in the observed bathochromic shift of the fluorescence spectra. The red shift also enables a ratiometric fluorescence measurement of the metal ions. **BDP-TPY** showed a sharp and strong absorption band around 515 nm ($\varepsilon = 51000$) (Table S2). Upon addition of heavy or transition-metal ions, the absorption spectra showed bathochromic shifts. In particular, the absorption band of **BDP-TPY** at 515 nm underwent a large shift to 543 nm upon addition of $Cu^{2+}$. The complex of **BDP-TPY** with $Fe^{2+}$ and $Fe^{3+}$ showed two absorption peaks around 513 and 640 nm (Table S2).

The $Zn^{2+}$-concentration-dependent fluorescence spectra of **BDP-TPY** are shown in Figure 5. Fluorescence spectra of **BDP-TPY** upon titration with $Zn^{2+}$ displayed a bathochromic fluorescence shift from 539 to 567 nm and a distinct ratiometric change with a clear isoemission point at 551 nm. The quantum yield changed from 0.91 to 0.66. The spectral change was largely terminated by the addition of 10 equiv of $Zn^{2+}$. Similar changes were observed in the absorption spectra. The maximum absorbance shifted bathochromically from 515 to 534 nm with an isosbestic point at 525 nm as the $Zn^{2+}$ concentration was increased in the solution (Table S2). Since $F_{567}$ increased while $F_{539}$ simultaneously decreased with increasing concentration of $Zn^{2+}$, the ratio of fluorescence intensities at the 567 and 539 nm ($F_{567}/F_{539}$) increased in response to changes in the $Zn^{2+}$ concentration (Figure 5). When the $Zn^{2+}$ concentration

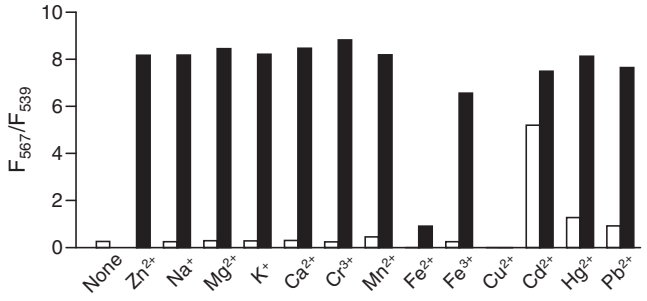


**Figure 6.** Changes of the fluorescence intensity ratio ($F_{567}/F_{539}$) of **BDP-TPY** upon addition of different metal ions. Spectra were acquired in aqueous acetonitrile solution (acetonitrile/water = 9/1, v/v). White bars represent the addition of an excess of the appropriate metal ion (1 mM for $Na^+$, $Mg^{2+}$, $K^+$, and $Ca^{2+}$. 10 μM for all other ions) to a 1 μM solution of **BDP-TPY**. Black bars represent the subsequent addition of 10 μM of $Zn^{2+}$ to the solution. Excitation was provided at 535 nm.

was 10 μM (i.e., 10 equiv), $F_{567}/F_{539}$ was 8.0. The fluorescence color changed from greenish-yellow to orange. The sigmoidal plot gives a quantitative determination of $Zn^{2+}$. The LOD and LOQ of **BDP-TPY** for $Zn^{2+}$ were $5.1 \times 10^{-9}$ and $1.7 \times 10^{-8}$ M, respectively. These values are sufficiently low for the detection in the submicromolar concentration range of $Zn^{2+}$ in many environmental, chemical, and biological systems. Job's plot[43] suggested a 1:1 complex of **BDP-TPY** with $Zn^{2+}$ (Figure S3). In addition, the observation of the isoemissive point in Figure 5 also indicates the formation of only one type of complex in this system. Therefore, Benesi–Hildebrand plots were used to determine a binding constant, which was $4.64 \times 10^5\ M^{-1}$ for $Zn^{2+}$ in the solution (Figure S3).

Competition experiments of $Zn^{2+}$ with some common ions were conducted to evaluate the selectivity of **BDP-TPY** toward $Zn^{2+}$ (Figure 6). The fluorescence intensity ratio ($F_{567}/F_{539}$) did not change upon addition of $Na^+$, $Mg^{2+}$, $K^+$, $Ca^{2+}$, $Cr^{3+}$, $Mn^{2+}$, and $Fe^{3+}$ to the solution of **BDP-TPY**. The signal increased slightly for $Hg^{2+}$ and $Pb^{2+}$ solutions, whereas it increased up to 5.2 for the $Cd^{2+}$ solution. Further addition of $Zn^{2+}$ to the solutions resulted in further increases in the signal. This result demonstrated that **BDP-TPY** preferentially binds to $Zn^{2+}$ rather than $Cd^{2+}$ or $Hg^{2+}$. Other research also reported that terpyridine shows good affinity for $Zn^{2+}$.[11,26,27,40]

The pH dependency of **BDP-TPY** was also investigated. In the pH range between 5.0 and 9.0, the fluorescence spectra of **BDP-TPY** were unchanged while the fluorescence intensity declined, with no spectral shift at pH 3 (Figure S4), and this might be attributed to diprotonation of the terpyridine.[11,44]

## Conclusion

In this study, two types of metal-ion receptor were directly linked to the 3 position of the BODIPY core using the Suzuki–Miyaura cross-coupling reaction. The fluoroionophores showed opposite wavelength responses toward heavy metal ions. The fluoroionophores responded to several heavy metal ions with specific fluorescence spectra that depend on the nature of the ionic species. Concentrations of $Cr^{3+}$ and $Zn^{2+}$ were successfully determined using a ratiometric fluorescence method. Only by changing the ion-receptor moiety could we modulate the wavelength-response characteristics and ion selectivity of the fluoroionophores, which is beneficial for the simultaneous analysis of several metal ions. In a future study, we will immobilize the fluoroionophores onto a solid support, which is applicable as a fluorescence sensor for environmental aqueous samples. In addition, Determination of $Zn^{2+}$ in roadway drainage by using **BDP-TPY** is now under way.

## Experimental

**Synthetic Materials and Methods.** Unless otherwise stated, all reagents were purchased from commercial suppliers and used without further purification. Reactions were monitored using high-performance thin-layer chromatography (HPTLC; silica gel 60 $F_{254}$, Merck, Germany) or thin-layer chromatography (TLC; aluminum oxide 60 $F_{254}$, basic, Merck, Germany). HPTLC plates were visualized in UV light and/or by staining with *p*-methoxybenzaldehyde–$H_2SO_4$–MeOH (1:2:17, v/v) followed by heating for a few minutes. Open-column chromatography was performed using silica gel 60 (230–400 mesh) or aluminum oxide 90 active basic. $^1H$ and $^{13}C$ spectra were recorded on a JEOL 400 (400 MHz $^1H$; 100 MHz $^{13}C$) spectrometer at room temperature. Chemical shifts are reported in ppm relative to tetramethylsilane (TMS) as the internal standard (residual $CHCl_3$; $^1H$ NMR 7.26 ppm, $^{13}C$ NMR 77.2 ppm). Coupling constants (*J*) were reported in hertz. Splitting patterns are indicated as s, singlet; d, doublet; t, triplet; q, quartet; m, multiplet; brs, broad singlet for $^1H$ NMR data. ESI high-resolution mass spectra (HRMS) were recorded on a Thermo Scientific Exactive spectrometer or JMS-T100LP spectrometer. FD HRMS spectra were recorded on JEOL JMS-T100GCv spectrometer.

**(4-Iodophenyl)bis(pyridin-2-ylmethyl)amine.** 4-Iodoaniline (500 mg, 2.28 mmol), 2-(bromomethyl)pyridine hydrobromide (1.73 g, 6.85 mmol), and potassium carbonate (947 mg, 6.85 mmol) were dissolved in DMF (12 mL) purged with $N_2$ in a 25-mL round flask. The reaction mixture was stirred at 70 °C for 3 h. After being cooled to room temperature, $CH_2Cl_2$ was added and the mixture was washed with $H_2O$, saturated aqueous (st. aq.) $NaHCO_3$, and brine, then dried ($Na_2SO_4$), and concentrated. The crude product was purified by column chromatography on silica gel ($CH_2Cl_2$/acetone = 5/1) to yield 302 mg (0.75 mmol, 33%) of (4-iodophenyl)bis(pyridin-2-ylmethyl)amine as a light brown solid. $^1H$ NMR (400 MHz, $CDCl_3$): $\delta$ 8.59 (d, 2H, $J = 4.8$ Hz), 7.63 (td, 2H, $J = 7.7$, 1.8 Hz), 7.39 (d, 2H, $J = 9.2$ Hz), 7.22–7.16 (m, 4H), 6.48 (d, 2H, $J = 9.1$ Hz), 3.98 (s, 4H); $^{13}C$ NMR (100 MHz, $CDCl_3$): $\delta$ 158.0, 149.6, 149.5, 137.6, 136.7, 122.0, 120.6, 114.7, 78.2, 57.3; HRMS (ESI) *m/z* calcd for $[M + H]^+$ $C_{18}H_{16}N_3IH$ 402.0462; found 402.0461.

**4-(2-Butyloctyloxy)-1,5-dihydropyrrol-2-one (3).** Compound **2**[45] (2.0 g, 17.7 mmol) was dissolved in 2-butyl-1-octanol (20 mL, 89.4 mmol) and the solution was warmed to 80 °C. Methanesulfonic acid (0.1 mL, 1.8 mmol) was slowly added to the solution, and then the mixture was stirred at this temperature for 24 h under vacuum. After being cooled to room temperature, the solution was filtered and then diluted with $CH_2Cl_2$. The filtrate was successively washed with $H_2O$, saturated aqueous (sat. aq.) $NaHCO_3$, and brine, and then dried

($Na_2SO_4$), and concentrated. The crude product was purified by column chromatography on silica gel ($CHCl_3$/EtOAc = 3/1) to yield 3.9 g (14.6 mmol, 82%) of **3** as a white solid. $^1$H NMR (400 MHz, $CDCl_3$): $\delta$ 6.42 (brs, 1H), 5.02 (s, 1H), 3.92 (s, 2H), 3.82 (d, 2H, $J$ = 5.6 Hz), 1.78–1.71 (m, 1H), 1.34–1.28 (m, 16H), 0.92–0.87 (m, 6H); $^{13}$C NMR (100 MHz, $CDCl_3$): $\delta$ 175.8, 175.1, 94.0, 74.3, 46.9, 37.4, 31.8, 31.1, 30.8, 29.5, 28.9, 26.7, 22.9, 22.6, 14.1, 14.0; HRMS (ESI) $m/z$ calcd for $[M + Na]^+$ $C_{16}H_{29}NO_2Na$ 290.2096; found 290.2092.

**4-(2-Butyloctyloxy)-5-(3,5-dimethyl-1*H*-pyrrol-2-ylmethylene)-1,5-dihydropyrrol-2-one (5).** Compound **3** (1.6 g, 6.1 mmol) and compound **4**[46] (0.5 g, 4.1 mmol) were dissolved in hexamethylphosphoric triamide (8 mL) and the solution was warmed to 70 °C. A 3 M NaOH (10 mL) solution was slowly added to the reaction mixture and stirred for 12 h. After being cooled to room temperature, the mixture was diluted with EtOAc and successively washed with $H_2O$, then dried ($Na_2SO_4$), and concentrated. The crude product was purified by column chromatography on silica gel ($CH_2Cl_2$/EtOAc = 10/1) to yield 0.9 g (2.5 mmol, 62%) of **5** as a yellow solid. $^1$H NMR (400 MHz, $CDCl_3$): $\delta$ 10.93 (s, 1H), 10.37 (s, 1H), 6.35 (s, 1H), 5.81 (s, 1H), 5.05 (s, 1H), 3.90 (d, 2H, $J$ = 5.8 Hz), 2.39 (s, 3H), 2.16 (s, 3H), 1.86–1.82 (m, 1H), 1.40–1.29 (m, 16H), 0.91–0.86 (m, 6H); $^{13}$C NMR (100 MHz, $CDCl_3$): $\delta$ 173.2, 167.0, 134.5, 126.7, 122.4, 121.9, 109.9, 100.0, 89.6, 74.3, 37.5, 31.8, 31.5, 31.2, 29.6, 29.0, 26.8, 23.0, 22.7, 14.1, 14.0, 13.1, 11.3; HRMS (ESI) $m/z$ calcd for $[M + H]^+$ $C_{23}H_{36}N_2O_2H$ 373.2855; found 373.2861.

**Trifluoromethanesulfonic Acid 4-(2-Butyloctyloxy)-5-(3,5-dimethyl-1*H*-pyrrol-2-ylmethylene)-5*H*-pyrrol-2-yl Ester (1).** $CH_2Cl_2$ (15 mL) was stirred into a solution of **5** (500 mg, 1.34 mmol) and triethylamine (0.56 mL, 4.03 mmol) at room temperature for 30 min under a nitrogen atmosphere. The reaction mixture was cooled to −78 °C, followed by addition of trifluoromethanesulfonic anhydride (0.68 mL, 4.03 mmol), and stirred at this temperature for 1 h. The reaction mixture was diluted with $CH_2Cl_2$ and successively washed with sat. aq. $NaHCO_3$ and brine, then dried ($Na_2SO_4$), and concentrated. The residue was purified by column chromatography on silica gel (hexane/EtOAc = 30:1) to yield 583 mg (1.15 mmol, 86%) of **1** as a brown oil. $^1$H NMR (400 MHz, $CDCl_3$): $\delta$ 10.68 (brs, 1H), 7.03 (s, 1H), 5.87 (s, 1H), 5.37 (s, 1H), 3.88 (d, 2H, $J$ = 5.8 Hz), 2.33 (s, 3H), 2.22 (s, 3H), 1.85–1.79 (m, 1H), 1.40–1.29 (m, 16H), 0.93–0.87 (m, 6H); $^{13}$C NMR (100 MHz, $CDCl_3$): $\delta$ 166.6, 160.2, 140.0, 134.3, 131.0, 126.7, 123.4, 120.2, 119.0, 117.0, 113.8, 112.3, 86.6, 74.9, 37.6, 31.8, 31.4, 31.1, 29.6, 29.0, 26.8, 23.0, 22.7, 14.1, 14.1, 13.8, 11.3; HRMS (ESI) $m/z$ calcd for $[M + H]^+$ $C_{24}H_{35}F_3N_2O_4SH$ 505.2348; found 505.2346.

**[4-(5,5-Dimethyl-1,3,2-dioxaboran-2-yl)phenyl]bis(pyridin-2-ylmethyl)amine (6).** (4-Iodophenyl)bis(pyridin-2-ylmethyl)amine (297 mg, 0.74 mmol), bis(2,2-dimethyl-1,3-propylidenedioxy)diborane (170 mg, 0.75 mmol), potassium acetate (218 mg, 2.22 mmol), and [1,1′-Bis(diphenylphosphino)ferrocene]palladium(II) dichloride dichloromethane adduct (18 mg, 0.02 mmol) were dissolved in DMF (6 mL) purged with $N_2$ in a 25-mL round flask. The reaction mixture was stirred at 80 °C for 5 h. After being cooled to room temperature, the reaction mixture was quenched by addition of $H_2O$, and then EtOAc was added. The organic layer was separated. The aqueous layer was washed with EtOAc twice. The combined organic layer was successively washed with $H_2O$ and brine, then dried ($Na_2SO_4$), and concentrated. The crude product was purified by column chromatography on aluminum oxide basic ($CHCl_3$/EtOAc = 15/1) to yield 180 mg (0.46 mmol, 63%) of **6** as a brown solid. $^1$H NMR (400 MHz, $CDCl_3$): $\delta$ 8.58 (d, 2H, $J$ = 4.1 Hz), 7.62–7.58 (m, 4H), 7.23 (d, 2H, $J$ = 7.9 Hz), 7.16 (dd, 2H, $J$ = 7.4, 4.9 Hz), 6.68 (d, 2H, $J$ = 8.8 Hz), 4.84 (s, 4H), 3.70 (s, 4H), 0.98 (s, 6H); $^{13}$C NMR (100 MHz, $CDCl_3$): $\delta$ 158.3, 149.9, 149.5, 136.6, 135.2, 121.9, 120.6, 111.4, 72.1, 56.9, 31.8, 21.9; HRMS (FD) $m/z$ calcd for $[M]^+$ $C_{23}H_{26}BN_3O_2$ 387.2118; found 387.2260.

**4-[4-(2-Butyloctyloxy)-5-(3,5-dimethyl-1*H*-pyrrol-2-ylmethylene)-5*H*-pyrrol-2-yl]phenylbis(pyridin-2-ylmethyl)amine (7).** Compound **1** (116 mg, 0.23 mmol), compound **6** (89 mg, 0.23 mmol), sodium carbonate (73 mg, 0.69 mmol), and tetrakis(triphenylphosphine)palladium(0) (8 mg, 0.01 mmol) were dissolved in toluene (8 mL) and MeOH (5 mL) purged with $N_2$ in a 25-mL round flask. The reaction mixture was refluxed for 17 h with stirring. After being cooled to room temperature, the reaction mixture was quenched by addition of $H_2O$, and then EtOAc was added. The organic layer was separated. The aqueous layer was washed with EtOAc twice. The combined organic layer was successively washed with $H_2O$ and brine, then dried ($Na_2SO_4$), and concentrated. The crude product was purified by column chromatography on silica gel ($CHCl_3$/EtOAc = 30/1) to yield 69 mg (0.11 mmol, 48%) of **7** as a red solid. $^1$H NMR (400 MHz, $CDCl_3$): $\delta$ 9.09 (br, 1H), 8.61 (d, 2H, $J$ = 4.0 Hz), 7.82 (d, 2H, $J$ = 8.9 Hz), 7.63 (td, 2H, $J$ = 7.7, 1.8 Hz), 7.26 (d, 2H, $J$ = 7.9 Hz), 7.20–7.17 (m, 2H), 6.81 (s, 1H), 6.77 (d, 2H, $J$ = 9.0 Hz), 5.95 (s, 1H), 5.81 (s, 1H), 4.90 (s, 4H), 3.90 (d, 2H, $J$ = 5.9 Hz), 2.33 (s, 3H), 2.21 (s, 3H), 1.88–1.82 (m, 1H), 1.41–1.29 (m, 16H), 0.93–0.86 (m, 6H); $^{13}$C NMR (100 MHz, $CDCl_3$): $\delta$ 167.0, 164.6, 158.1, 149.6, 149.0, 140.2, 136.7, 136.5, 129.8, 128.1, 128.0, 124.4, 122.0, 120.7, 113.1, 112.2, 111.1, 94.1, 74.2, 57.2, 37.6, 31.8, 31.5, 31.2, 29.6, 29.0, 26.8, 23.0, 22.6, 14.1, 14.1, 13.9, 11.2; HRMS (ESI) $m/z$ calcd for $[M + H]^+$ $C_{41}H_{51}N_5OH$ 630.4166; found 630.4166.

**1-(2-Butyloctyloxy)-5,7-dimethyl-3-[4-bis(pyridin-2-ylmethyl)aminophenyl]-4,4-difluoro-3a,4a-diaza-4-bora-*s*-indacene (BDP-DPA).** A solution of compound **7** (72 mg, 0.11 mmol), boron trifluoride etherate (72 μL, 0.57 mmol), and triethylamine (48 μL, 0.34 mmol) was stirred in anhydrous toluene (30 mL) at room temperature under a nitrogen atmosphere. The reaction mixture was warmed to 115 °C and stirred for 19 h. After being cooled to room temperature, $CH_2Cl_2$ was added and the mixture was washed with $H_2O$, sat. aq. $NaHCO_3$, and brine, then dried ($Na_2SO_4$), and concentrated. The crude product was purified by column chromatography on silica gel (hexane/EtOAc = 1/1) to yield 63 mg (0.09 mmol, 81%) of **BDP-DPA** as a purple solid. $^1$H NMR (400 MHz, $CDCl_3$): $\delta$ 8.60 (d, 2H, $J$ = 4.0 Hz), 7.88 (d, 2H, $J$ = 9.9 Hz), 7.64 (td, 2H, $J$ = 7.7, 1.8 Hz), 7.27 (d, 2H, $J$ = 7.4 Hz), 7.20–7.17 (m, 2H), 7.10 (s, 1H), 6.77 (d, 2H, $J$ = 9.0 Hz), 5.99 (s, 1H), 5.91 (s, 1H), 4.88 (s, 4H), 3.95 (d, 2H, $J$ = 5.8 Hz), 2.47 (s, 3H), 2.23 (s, 3H), 1.86–1.80 (m, 1H), 1.41–1.29 (m, 16H), 0.93–0.86 (m, 6H); $^{13}$C NMR (100 MHz, $CDCl_3$): $\delta$ 162.4, 158.2, 157.9, 152.2, 149.6, 149.4, 137.2,

136.7, 131.1, 130.8, 126.9, 122.0, 120.9, 120.6, 117.6, 116.3, 111.9, 98.4, 74.3, 56.9, 37.6, 31.8, 31.3, 31.0, 29.6, 29.0, 26.7, 23.0, 22.6, 14.6, 14.1, 14.1, 11.2; HRMS (ESI) $m/z$ calcd for $[M + Na]^+$ $C_{41}H_{50}BF_2N_5ONa$ 699.4005; found 699.4017.

**4′-[4-(2-Butyloctyloxy)-5-(3,5-dimethyl-1*H*-pyrrol-2-ylmethylene)-5*H*-pyrrol-2-yl]-2,2′:6′,2″-terpyridine (9).** Compound **1** (128 mg, 0.25 mmol), compound **8**[47] (92 mg, 0.27 mmol), cesium fluoride (116 mg, 0.76 mmol), and tetrakis(triphenylphosphine)palladium(0) (29 mg, 0.03 mmol) were dissolved in 1,4-dioxane (8 mL) purged with $N_2$ in a 25-mL round flask. The reaction mixture was refluxed for 1 h with stirring. After being cooled to room temperature, the reaction mixture was quenched by addition of $H_2O$, and then $CH_2Cl_2$ was added. The organic layer was separated. The aqueous layer was washed with $CH_2Cl_2$ twice. The combined organic layer was successively washed with $H_2O$ and brine, then dried ($Na_2SO_4$), and concentrated. The crude product was purified by column chromatography on aluminum oxide basic (hexane/EtOAc = 7/1) to yield 18 mg (0.03 mmol, 12%) of **9** as an orange solid. $^1$H NMR (400 MHz, $CDCl_3$): $\delta$ 8.99 (s, 2H), 8.74 (d, 2H, $J = 3.9$ Hz), 8.66 (d, 2H, $J = 7.9$ Hz), 7.87 (td, 2H, $J = 7.7$, 1.8 Hz), 7.36–7.32 (m, 2H), 7.05 (s, 1H), 6.33 (s, 1H), 5.91 (s, 1H), 3.98 (d, 2H, $J = 5.9$ Hz), 2.47 (s, 3H), 2.27 (s, 3H), 1.90–1.86 (m, 1H), 1.43–1.31 (m, 16H), 0.96–0.88 (m, 6H); $^{13}$C NMR (100 MHz, $CDCl_3$): $\delta$ 166.7, 160.9, 156.2, 155.6, 148.9, 144.1, 141.0, 138.8, 136.6, 134.0, 129.1, 123.5, 121.1, 117.8, 117.4, 112.6, 94.9, 74.5, 37.7, 31.8, 31.5, 31.2, 29.7, 29.1, 26.8, 23.0, 22.7, 14.2, 14.1, 14.1, 11.4; HRMS (ESI) $m/z$ calcd for $[M + H]^+$ $C_{38}H_{45}N_5OH$ 588.3697; found 588.3700.

**1-(2-Butyloctyloxy)-5,7-dimethyl-3-(4′-2,2′:6′,2″-terpyridinyl)-4,4-difluoro-4-bora-3a,4a-diaza-*s*-indacene (BDP-TPY).** A solution of compound **9** (109 mg, 0.19 mmol), boron trifluoride etherate (117 μL, 0.93 mmol), and triethylamine (77 μL, 0.56 mmol) was stirred in anhydrous toluene (30 mL) at room temperature under a nitrogen atmosphere. The reaction mixture was warmed to 130 °C with stirring for 3 h under nitrogen. After being cooled to room temperature, $CH_2Cl_2$ was added and the mixture was washed with $H_2O$, sat. aq. $NaHCO_3$, and brine, then dried ($Na_2SO_4$), and concentrated. The crude product was purified by column chromatography on aluminum oxide basic (hexane/EtOAc = 6/1) to yield 51 mg (2.5 mmol, 62%) of **BDP-TPY** as a dark purple solid. $^1$H NMR (400 MHz, $CDCl_3$): $\delta$ 8.89 (s, 2H), 8.74 (d, 2H, $J = 4.2$ Hz), 8.62 (d, 2H, $J = 8.1$ Hz), 7.86 (td, 2H, $J = 7.7$, 1.8 Hz), 7.35–7.31 (m, 2H), 7.29 (s, 1H), 6.21 (s, 1H), 6.07 (s, 1H), 4.03 (d, 2H, $J = 5.9$ Hz), 2.49 (s, 3H), 2.29 (s, 3H), 1.90–1.84 (m, 1H), 1.46–1.31 (m, 16H), 0.96–0.88 (m, 6H); $^{13}$C NMR (100 MHz, $CDCl_3$): $\delta$ 161.5, 157.5, 156.1, 155.5, 153.1, 149.1, 142.2, 141.3, 136.6, 133.1, 125.6, 123.5, 121.4, 120.6, 119.5, 119.0, 100.1, 74.7, 37.7, 31.8, 31.3, 31.0, 29.6, 29.0, 26.8, 23.0, 22.7, 15.0, 14.1, 14.1, 11.3; HRMS (ESI) $m/z$ calcd for $[M + Na]^+$ $C_{38}H_{44}BF_2N_5ONa$ 658.3499; found 658.3509.

**Spectroscopic Measurements.** The spectroscopic measurements were carried out in an aqueous acetonitrile solution ($CH_3CN/H_2O = 9/1$, v/v). Stock solutions of fluoroionophores were prepared by dissolving each fluoroionophore in analytical grade acetonitrile. Stock solutions of metal ions were prepared by dissolving appropriate amounts of analytical grade perchlorate salts in a Tris-HCl buffer (0.01 M). Mill-Q water (18.25 MΩ cm) was used to prepare all aqueous solutions. Quartz cells (cross section of 1 cm × 1 cm) were used for fluorescence and absorption measurements. Fluorescence and absorption spectra were obtained on a JASCO FP-6600 spectrofluorometer and a JASCO V-630 spectrophotometer, respectively. The excitation and fluorescence slit widths were 5.0 and 6.0 nm, respectively. A detection limit (LOD, $3\sigma$/slope) and a quantification limit (LOQ, $10\sigma$/slope) for each metal ion were determined based on the standard deviation ($\sigma$) of 11 blank solutions.[48]

**Determination of the Fluorescence Quantum Yield.** The relative quantum yields of the samples were obtained by comparing the area under the corrected fluorescence spectrum of the test sample with that of a solution of Rhodamine 6G in $H_2O$, which has a reported quantum yield of 0.76.[49] The quantum yields of fluorescence ($\Phi_S$) were obtained from multiple measurements ($N = 3$) with the following equation:

$$\Phi_S = \Phi_R \times S_S/S_R \times A_R/A_S \times (\eta_S/\eta_R)^2 \quad (1)$$

where $\Phi$ is the quantum yield, $S$ is the integrated area of the corresponding fluorescence spectrum, $A$ is the absorbance at the excitation wavelength, $\eta$ is the refractive index of the solvent used, and the subscripts S and R refer to the sample and the reference fluorophore, respectively.

This research was financially supported by Core Research of Evolutional Science & Technology (CREST) for "Innovative Technology and Systems for Sustainable Water Use" from Japan Science and Technology Agency (JST). This study was also partially supported by Grants-in-Aid for Scientific Research (No. 23686074) from Japan Society for the Promotion of Science.

## Supporting Information

Additional fluorescence and absorption spectra of fluoroionophores, $^1$H NMR, $^{13}$C NMR, and mass spectra of all new compounds. This material is available free of charge on the Web at: http://www.csj.jp/journals/bcsj/.

## References

1 K. Kawata, H. Yokoo, R. Shimazaki, S. Okabe, *Environ. Sci. Technol.* **2007**, *41*, 3769.

2 D. A. Eastmond, J. T. MacGregor, R. S. Slesinski, *Crit. Rev. Toxicol.* **2008**, *38*, 173.

3 D. Mohan, C. U. Pittman, Jr., *J. Hazard. Mater.* **2006**, *137*, 762.

4 W. Naito, M. Kamo, K. Tsushima, Y. Iwasaki, *Sci. Total Environ.* **2010**, *408*, 4271.

5 H. Deng, Z. H. Ye, M. H. Wong, *Environ. Pollut.* **2004**, *132*, 29.

6 Z. Wang, D.-M. Fang, Q. Li, L.-X. Zhang, R. Qian, Y. Zhu, H.-Y. Qu, Y.-P. Du, *Anal. Chim. Acta* **2012**, *725*, 81.

7 A. E. Shiel, J. Barling, K. J. Orians, D. Weis, *Anal. Chim. Acta* **2009**, *633*, 29.

8 *Principles of Fluorescence Spectroscopy*, 3rd ed., ed. by J. R. Lakowicz, Springer, New York, **2006**. doi:10.1007/978-0-387-46312-4.

9 F. A. Khan, K. Parasuraman, K. K. Sadhu, *Chem. Commun.*

**2009**, 2399.
10 Z. Xu, S. J. Han, C. Lee, J. Yoon, D. R. Spring, *Chem. Commun.* **2010**, *46*, 1679.
11 Z. Yang, C. Yan, Y. Chen, C. Zhu, C. Zhang, X. Dong, W. Yang, Z. Guo, Y. Lu, W. He, *Dalton Trans.* **2011**, *40*, 2173.
12 B. Valeur, *Molecular Fluorescence: Principles and Applications*, Wiley-VCH, Weinheim, **2001**. doi:10.1002/3527600248.
13 R. P. Haugland, *The Molecular Probes Handbook: A Guide to Fluorescent Probes and Labeling Technologies*, 11th ed., Molecular Probes, Inc., Eugene, **2010**.
14 A. Loudet, K. Burgess, *Chem. Rev.* **2007**, *107*, 4891.
15 K. Yamada, Y. Nomura, D. Citterio, N. Iwasawa, K. Suzuki, *J. Am. Chem. Soc.* **2005**, *127*, 6956.
16 M. Baruah, W. Qin, R. A. L. Vallée, D. Beljonne, T. Rohand, W. Dehaen, N. Boens, *Org. Lett.* **2005**, *7*, 4377.
17 X. Peng, J. Du, J. Fan, J. Wang, Y. Wu, J. Zhao, S. Sun, T. Xu, *J. Am. Chem. Soc.* **2007**, *129*, 1500.
18 Y. Ando, S. Iino, K. Yamada, K. Umezawa, N. Iwasawa, D. Citterio, K. Suzuki, *Sens. Actuators, B* **2007**, *121*, 74.
19 D. W. Domaille, L. Zeng, C. J. Chang, *J. Am. Chem. Soc.* **2010**, *132*, 1194.
20 O. A. Bozdemir, R. Guliyev, O. Buyukcakir, S. Selcuk, S. Kolemen, G. Gulseren, T. Nalbantoglu, H. Boyaci, E. U. Akkaya, *J. Am. Chem. Soc.* **2010**, *132*, 8029.
21 H. Son, H. Y. Lee, J. M. Lim, D. Kang, W. S. Han, S. S. Lee, J. H. Jung, *Chem.—Eur. J.* **2010**, *16*, 11549.
22 D. Wang, Y. Shiraishi, T. Hirai, *Tetrahedron Lett.* **2010**, *51*, 2545.
23 Z. Liu, C. Zhang, W. He, Z. Yang, X. Gao, Z. Guo, *Chem. Commun.* **2010**, *46*, 6138.
24 X.-B. Yang, B.-X. Yang, J.-F. Ge, Y.-J. Xu, Q.-F. Xu, J. Liang, J.-M. Lu, *Org. Lett.* **2011**, *13*, 2710.
25 Y. Shiraishi, C. Ichimura, S. Sumiya, T. Hirai, *Chem.—Eur. J.* **2011**, *17*, 8324.
26 W. Goodall, J. A. G. Williams, *Chem. Commun.* **2001**, 2514.
27 X. Piao, Y. Zou, J. Wu, C. Li, T. Yi, *Org. Lett.* **2009**, *11*, 3818.
28 M. Glasbeek, H. Zhang, *Chem. Rev.* **2004**, *104*, 1929.
29 Z. Zhou, M. Yu, H. Yang, K. Huang, F. Li, T. Yi, C. Huang, *Chem. Commun.* **2008**, 3387.
30 H. A. Benesi, J. H. Hildebrand, *J. Am. Chem. Soc.* **1949**, *71*, 2703.
31 M. Sarkar, S. Banthia, A. Samanta, *Tetrahedron Lett.* **2006**, *47*, 7575.
32 J. Mao, L. Wang, W. Dou, X. Tang, Y. Yan, W. Liu, *Org. Lett.* **2007**, *9*, 4567.
33 K. Huang, H. Yang, Z. Zhou, M. Yu, F. Li, X. Gao, T. Yi, C. Huang, *Org. Lett.* **2008**, *10*, 2557.
34 A. J. Weerasinghe, C. Schmiesing, E. Sinn, *Tetrahedron Lett.* **2009**, *50*, 6407.
35 Y. Wan, Q. Guo, X. Wang, A. Xia, *Anal. Chim. Acta* **2010**, *665*, 215.
36 Y. Zheng, J. Orbulescu, X. Ji, F. M. Andreopoulos, S. M. Pham, R. M. Leblanc, *J. Am. Chem. Soc.* **2003**, *125*, 2680.
37 T. Hirano, K. Kikuchi, Y. Urano, T. Nagano, *J. Am. Chem. Soc.* **2002**, *124*, 6555.
38 Y. Wu, X. Peng, B. Guo, J. Fan, Z. Zhang, J. Wang, A. Cui, Y. Gao, *Org. Biomol. Chem.* **2005**, *3*, 1387.
39 J. Karolin, L. B.-A. Johansson, L. Strandberg, T. Ny, *J. Am. Chem. Soc.* **1994**, *116*, 7801.
40 C. Goze, G. Ulrich, L. Charbonnière, M. Cesario, T. Prangé, R. Ziessel, *Chem.—Eur. J.* **2003**, *9*, 3748.
41 A. Coskun, M. D. Yilmaz, E. U. Akkaya, *Org. Lett.* **2007**, *9*, 607.
42 E. Deniz, G. C. Isbasar, Ö. A. Bozdemir, L. T. Yildirim, A. Siemiarczuk, E. U. Akkaya, *Org. Lett.* **2008**, *10*, 3401.
43 K. A. Connars, *Binding Constants*, Wiley-Interscience, New York, **1987**.
44 U. Resch-Genger, Y. Q. Li, J. L. Bricks, V. Kharlanov, W. Rettig, *J. Phys. Chem. A* **2006**, *110*, 10956.
45 L. Duc, J. F. McGarrity, T. Meul, A. Warm, *Synthesis* **1992**, 391.
46 L. Wu, K. Burgess, *Chem. Commun.* **2008**, 4933.
47 C. J. Aspley, J. A. G. Williams, *New J. Chem.* **2001**, *25*, 1136.
48 Z.-X. Han, X.-B. Zhang, Z. Li, Y.-J. Gong, X.-Y. Wu, Z. Jin, C.-M. He, L.-X. Jian, J. Zhang, G.-L. Shen, R.-Q. Yu, *Anal. Chem.* **2010**, *82*, 3108.
49 J. Olmsted, *J. Phys. Chem.* **1979**, *83*, 2581.